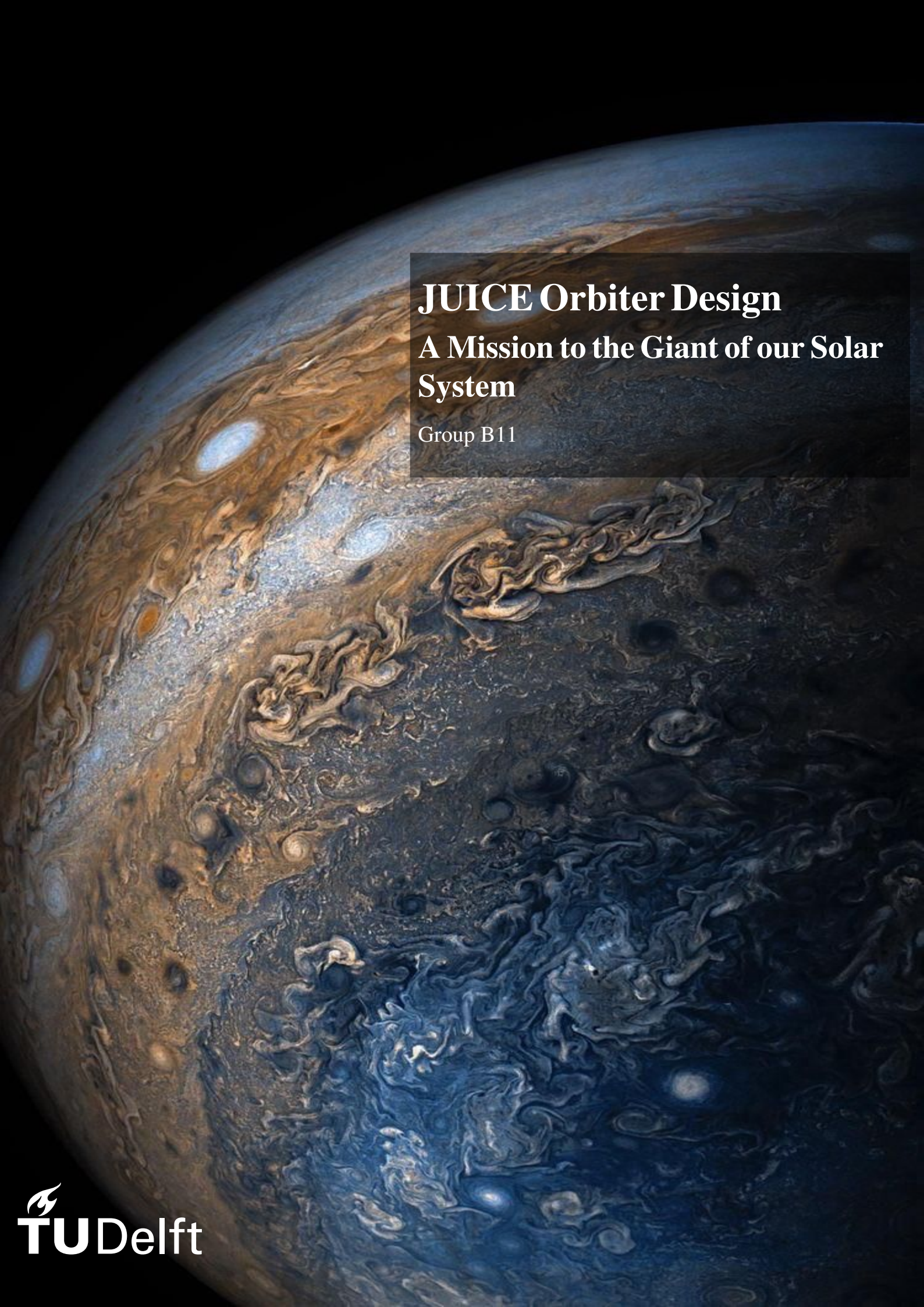

JUICE Orbiter Design

A Mission to the Giant of our Solar System

Group B11

TU Delft

DELFT UNIVERSITY OF TECHNOLOGY

FACULTY OF AEROSPACE ENGINEERING

AE2111-I

AEROSPACE SYSTEMS DESIGN

Design of the JUICE Spacecraft

A Mission to the Giant of our Solar System

Mission: Jupiter's JUICE mission
Lecturer: W.A. Timmer
Teaching Assistant: Lidia Rzeplińska

March 29, 2022

Group B11

Antonio Minafra	5027993	Sam Broos	4992873
Jonatan Valk	5028817	Silvano Tromp	5049237
Niklas Knöll	5006961	Stefano Kok	4656091
Lorenz Veithen	5075211	Tarek Abdelrazek	4993004

TU Delft Delft University of Technology

Summary

To carry the required propellants of the JUICE spacecraft, a fuel tank and oxidizer tank are required. This report describes the design process for both of these tanks, including a dynamic study to verify the spacecraft would stand up to launch. Finally, the risks associated with micrometeoroids were assessed.

Before starting with more detailed analysis, the required volume of each tank was calculated from previous work, from which the mounting system inside the spacecraft could be derived. Additionally, the loads from internal pressure and due to launch were calculated. The tanks' shape were assumed to be cylinders with spherical caps.

With these basic start parameters given, a design process was devised and implemented in Python. This design process first defined the minimum and maximum possible radii for the tanks, which would be possible to fit inside the spacecraft, as well as minimum and maximum thickness for the tank walls. For both variables, many steps in between the extreme values were taken and combined to form a design option. Each design option was evaluated to check if it would fail under different loads, where all the design options that did not fail were saved for later evaluation.

The procedure was followed for multiple different materials for both the fuel and oxidizer tanks. This resulted in multiple designs of different materials that would stand up to the forces and requirements placed on the tanks. For each material the lightest possible of these designs was selected, which were then traded off on the criteria of mass, cost and degradation during the mission. This led to a final selection of two titanium tanks for the oxidizer and fuel with the following dimensions as illustrated in Figure 1 and Table 1.

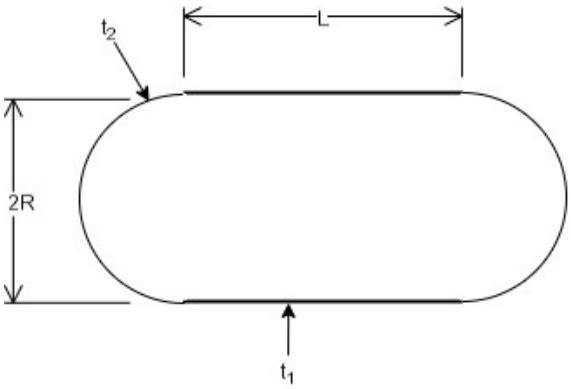

Figure 1: General Geometry with naming convention

Table 1: Results of tank designs

Geometry	**Oxidizer tank**	**Fuel tank**
R [m]	0.467	0.505
L [m]	0.045	0.044
t_1 [mm]	3.35	3.63
t_2 [mm]	1.33	1.44
Mass	22.7	27.4
Material	Titanium	Titanium
Material cost [$]	368.44	445.25

Following the design of the tank, a vibrational analysis of the tank and the spacecraft is performed. First the entire spacecraft was assumed to be a single mass attached to the launch vehicle, which resulted in natural frequencies of $17.36Hz$ and $78.44Hz$ for the lateral and longitudinal directions respectively. This satisfies the launcher requirements. The same study is performed for the tanks attached to the spacecraft, which results in a natural frequency of $191Hz$, which again is satisfactory. The two systems are now combined to form a two degree of freedom system and the equations of motion as well as the lowest natural frequency are determined. This lowest natural frequency again is satisfactory at $55.2Hz$. For the simple single degree of freedom system the frequency response when a periodic force is applied is analyzed. First the displacement over time is determined, followed by the amplitude depending on the frequency of the applied sinusoidal force. This analysis shows that the natural frequencies and responses to forcing are not a problem.

Finally the potential damage due to impacts of micrometeoroids that the spacecraft will encounter during its mission is assessed. To begin with the particles to be analyzed are selected. For the largest particle assessed

the particle size that has a 5% chance over the entire mission to impact the spacecraft is chosen. The smaller particle to be analyzed is one that is statistically certain to impact the spacecraft multiple times. Using an empirical formula the penetration depths in the spacecraft wall were calculated to be $8.168\ mm$ and $0.166\ mm$ for the larger and smaller particles respectively. From these results it was concluded that the larger particles pose a problem for the mission as it is currently designed, while the smaller particles cause only negligible damage. Thus it is recommended to implement some shielding, for example in the form of a whipple shield.

Contents

List of Symbols

Latin Letters	Quantity	Symbol Unit
a	Semi-major axis	km
A	Cross sectional area of cylindrical part	m
b	Semi-minor axis	km
D	Diameter	m
E	Modulus of elasticity	GPa
f	Frequency	Hz
f_f	Natural frequency fuel tank	Hz
f_n	Natural frequency	Hz
f_o	Natural frequency oxidizer tank	Hz
F_{lat}	Lateral force	N
$F_{res_{attach}}$	Resultant force acting on the attachment	N
$F_{res_{WP4}}$	Resultant force acting on the attachment from WP4	N
F_z	Axial force	N
g	Gravitational acceleration on Earth	$\frac{m}{s^2}$
I	Moment of inertia	m^4
k_{cr}	Value required for shell buckling	[-]
K_{Axial}	Axial spring constant	[-]
$K_{Lateral}$	Lateral spring constant	[-]
L	Length of the cylindrical part	m
L_p1	Length of the rod (ASS8)	m
L_p2	Length of the cantilever beam (ASS9)	m
m_{attach}	Mass of one attachment	kg
$m_{attach_{WP4}}$	Mass of one attachment from WP4	kg
m_p	projectile mass	g
M	Total spacecraft mass	kg
n_{attach}	Number of attachments	[-]
n_{lat}	Static lateral load factor	[-]
n_z	Static axial load factor	[-]
p	Internal pressure	Pa
Q	Dummy value used for computations	[-]
r_1		m
r_2		m
R	Radius of the cylinder and spherical part	m
t	Projectile penetration depth	cm
t_1	Thickness of the cylindrical part	m
t_2	Thickness of the spherical caps	m
v	Poisson ratio	[-]
v_p	impact velocity	km/s
V	Volume of the tank	m^3
t	Penetration Depth	mm
K	Material coefficient	[-]
m_p	Particle mass	g
v_p	Particle velocity	$\frac{km}{s}$
m_1	Mass of the spacecraft	kg
m_2	Mass of the tank	kg

k_1	axial spring constant of the spacecraft	N/m
k_2	axial spring constant of the tank	N/m

Greek Letters	**Quantity**	**Symbol Unit**
$\epsilon_{cylinder}$	strain of cylindrical section	[-]
ϵ_{sphere}	strain of spherical section	[-]
η	Efficiency	[-]
λ	Constant required for shell buckling analysis	[-]
μ	Standard gravitational parameter	km^3/s^2
ω	Angular velocity	rad/s
ω_{ox}	Angular velocity of oxidizer	rad/s
ω_f	Forcing angular frequency	rad/s
ω_{fuel}	Angular velocity of fuel tank	rad/s
ρ	Density	kg/m^3
ρ_p	Projectile density	g/cm^3
σ_p	Stress due to internal pressure	MPa
σ_{axial}	Total axial stress	MPa
σ_{cr}	Critical stress	MPa
σ_y	Yield stress	MPa

List of Figures

List of Tables

List of Abbreviations

DOF - *Degree of freedom*
FBD - *Free body diagram*
WP - *Work package*

Introduction 1

The Great Red Spot on Jupiter is a high pressure region that causes the largest storm in the entire solar system. According to historical observations it has persisted for at least 360 years, yet humanity does not understand how it is formed or what causes its colour. This is only one of the many aspects of Jupiter's atmosphere that is yet to be explored. Previously, there has only been one single Jupiter orbiter; Juno, which has provided great insights into Jupiter's composition, however a great amount of unknowns persist. This is the reason the European Space Agency is developing a new Jupiter orbiter called JUICE to further explore the natural phenomena present on Jupiter.

Any interplanetary spacecraft will need some way of performing maneuvers to arrive at the point of interest the mission is designed to study. There are a multitude of propulsion systems to perform such maneuvers, however the JUICE orbiter previously has been designed to use a chemical hydrazine propulsion system. For the required change in velocity to be able to reach Jupiter quite some volume of propellant is needed, which needs to be brought along and stored in the right conditions. Additionally, such large tanks that are required to store the fuel can at also be used to bear the load placed on the spacecraft, reducing the amount of mass needed for the structures.

This report details the design of such a tank system that stores both an oxidizer and hydrazine for the engine. In chapter 2 the tanks are designed to be able to generally be in the right shape to fit in the spacecraft with the other systems, as well as withstand the applied loads, such as the launch and internal pressure, without exceeding the yield strength of the chosen material or buckling. Afterwards, in chapter 3, a dynamical study is performed, in which the designed tanks and their attachments are used to find the natural frequencies of different configurations of the spacecraft. Finally, in chapter 4 the potential damage due to micrometeoroids that might impact the spacecraft during its mission is determined and whether mitigation for the possible damages is needed.

Fuel Tank Design 2

In this chapter, the design process of the fuel and oxidizer tank are given. First in Section 2.1 the design goals and requirements for the design are formulated. Then in Section 2.2 the preliminary layout of the design is constructed. From this a method is developed to iterate on the design, this is done in Section 2.3. Using the iteration technique multiple designs could be set up each featuring a different material. In Section 2.4.1 the designs are compared and a trade off is conducted to find the final design. Finally, in Section 2.5.4, the final design is summarized and CATIA models are made.

2.1 Design goals

In this section the design goals are established for the design are formulated to provide a guideline for the design process. The important goals are listed in the following list:

- The tank shall become part of the load carrying structure.
- The fuel tank shall not fail due to the internal pressure
- The tanks shall be linked to the body of the spacecraft without failure of any component
- The tanks shall not fail due to additional loads

2.2 Preliminary Layout

During the subsystem design phase, the general layout of the propellant tank and its dimensions were already determined. The volume of the fuel and the propellant were calculated from their densities using Equation 2.1, taking into account a safety margin of 10%.

$$V = \frac{1.1 \cdot M}{\rho} \tag{2.1}$$

The fuel ought to have a volume of $0.575\ m^3$ and the oxidizer of $0.456\ m^3$. However, contrary to the previous design [1], our current design now has one fuel tank and one oxidizer tank to reduce the complexity of the connections between the tanks, the primary structure and the structure between the two tanks themselves. Given that the radius and length of the spacecraft will not influence the design of the propellant tanks because of how much clearance there is, a fineness ratio of 1.25 has been used in order for the tanks to be designed for weight efficiency. Additionally, the lengths of both propellants are to be constant. [2]. Using 2.2 from [1] and using the volume of a sphere and a cylinder, these formulas are generated in order to check the radius required for the propellant tanks:

$$\frac{4}{3}\pi r_1^3 + \pi(0.5r_1)r^3 - 0.456 = 0 \tag{2.2}$$

$$\frac{4}{3}\pi r_2^3 + \pi(0.5r_1)r_2^3 - 0.575 = 0 \tag{2.3}$$

Equation 2.2 and Equation 2.3 compute the preliminary required radius and length for the tank design. These mentioned formulas do not take into account stresses or buckling and are purely based on the requirement of

volume, however in the coming sections further constraints are present, such as the Euler column buckling and the shell buckling, which will give more accurate results compared to the current preliminary results. Furthermore, according to Equation 2.2 and Equation 2.3 and the fact that the design (initially) has a fineness ratio of 1.25 gives the final values for the geometry of the tanks. The values are summarized in Table 2.2.

Table 2.1: Length and radius of the tanks

	Length	**Radius**
Oxidizer	0.215 m	0.43 m
Fuel	0.23 m	0.46 m

Rough sketch of the preliminary design

To get an idea of the design and the general layout some rough sketches were made using the preliminary geometrical results from Table 2.2. A sketch of the side view is given in Figure 2.1 and a sketch of the top view is given in Figure 2.2.

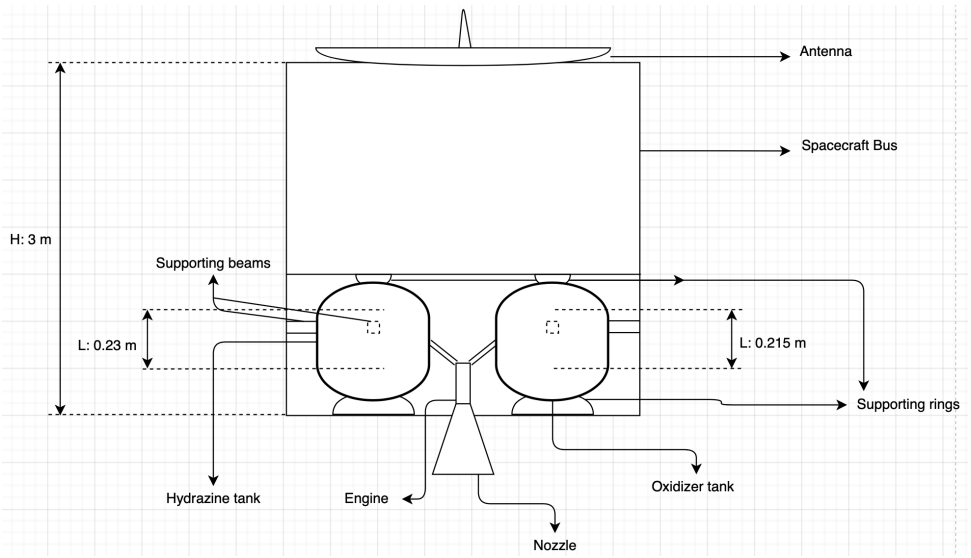

Figure 2.1: Side-view of the preliminary design

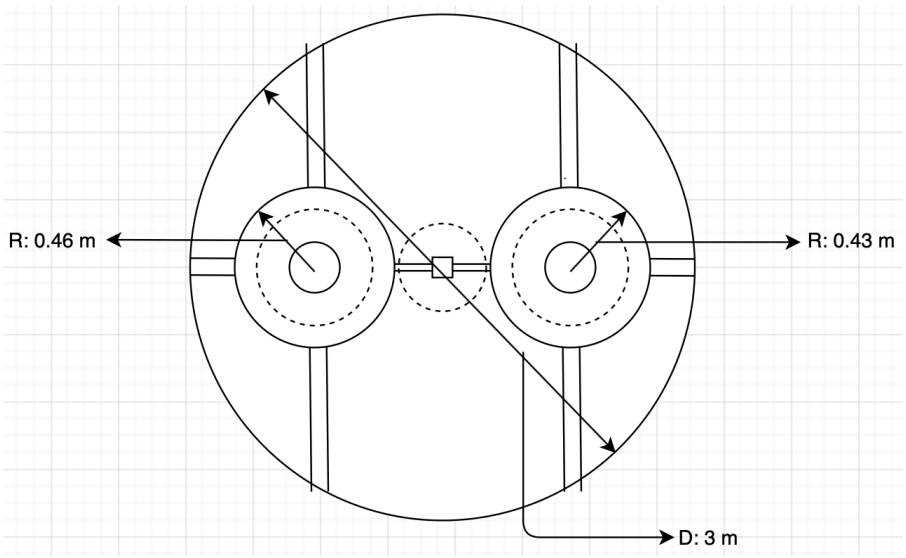

Figure 2.2: Top-view of the preliminary design

As can be deduced from the rough sketch, the propellant tank configuration consists of one oxidizer and one fuel tank. Although, both tanks have different dimensions, they do have one common shelve above them. This is realised by using four ring supports of minor different dimensions, to allow both tanks to have the same height and thus have a shelve on top. Moreover, as can be clearly seen from the top-view sketch, the tanks each have three square-shaped beam-connections to the vehicle wall. A connection between both tanks would be over-constraining the structure, thus the team chose not to include it. Together with the ring supports it creates enough support for the tanks to be kept in place.

Furthermore, both tanks are placed as close as possible to the engine and main thruster, in order to keep the propellant flow as short and efficient as possible. It also makes it possible to use the original connections that come with the engine, instead of elongating them.

Design Justification

The previous design created in WP2 was designed based on the stress caused by the pressure inside the tank and the volume requirement, additionally a shape of a sphere has been used in order for the tank to be more weight efficient [2]

To update the previous design, now a support structure for the propellant tanks has been chosen, in order to have a more stable and integrated design of the propellant system. Figure 2.1 and Figure 2.2 present the lay-out and design of the updated propellant system. The design that was chosen is inspired from the Juno propellant supporting structure. There are multiple reasons that led to choosing this design:

- The connection points of the tanks to the primary structure are well distributed, therefore the stresses are not concentrated in one point.
- Attaching the propellant tanks to various components like beams and the primary structure reduces the sloshing effects of the fuel.
- The tanks are oriented vertically so that the least amount of space is used.
- The shape of the spacecraft is kept as a cylinder as including corners in the body causes stress concentrations.
- It has been chosen to use 3 beams per tank to constrain the tanks in every direction. There is no fourth connecting beam to

2.3 Design Procedure

In this section, the design procedure is given. Using the procedure the best design can be found, this will be treated in Section 2.4.2. It is chosen to make the design procedure using Python. The main logic behind the Python code is presented in Figure 2.3.

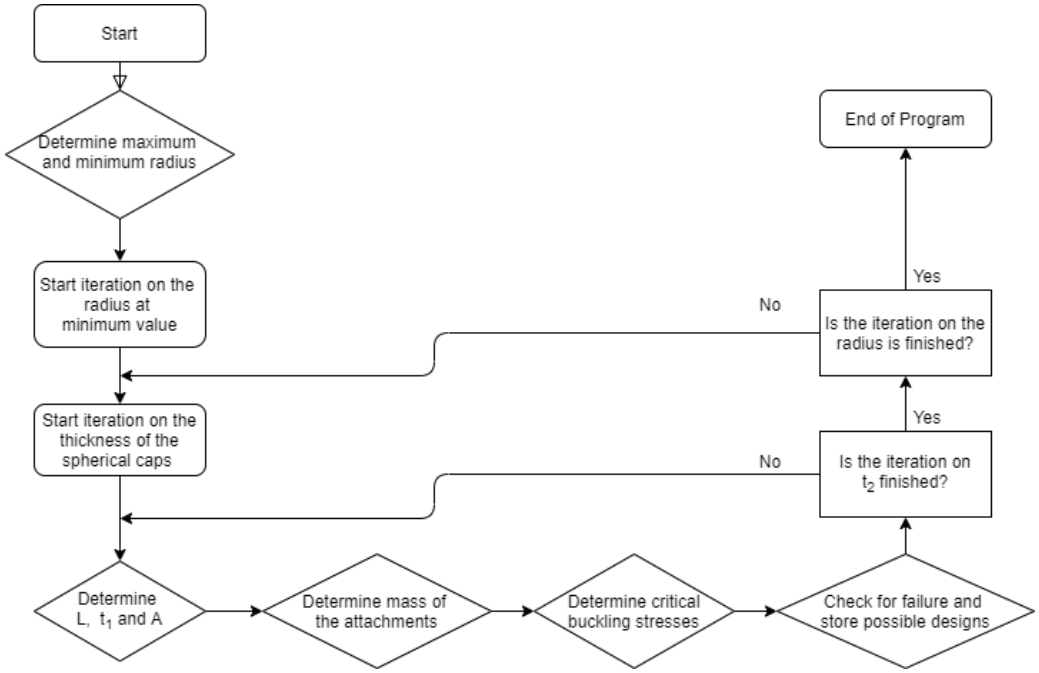

Figure 2.3: Flow chart of the iteration procedure

Once the program was run completely, a list of all the possible designs (non-failing ones) was returned. From there, the one providing the lowest mass was chosen. This method is not fully accurate because of the time constraint and the limitations of the equations used. All assumptions made during the development of this algorithm are listed in the following:

- $[ASS1]$ - A thin walled assumption was used for all calculations as all thicknesses are expected to respect the rule of thumb: $t \ll 0.1 \cdot R$ (or L depending on which one is the smallest).
- $[ASS2]$ - The volume of the fuel and oxidizer do not change significantly with respect to the obtained values from WP2 [1]. That is, no convergence procedure was used to take the changing volume of fuel and oxidizer (due to the slight change in structural mass) into account. This was decided in order to reduce the computational time and power required by the algorithm.
- $[ASS3]$ - The same values for the internal pressure of both oxidizer and fuel tanks from WP2 [1] were used. p = 25 bar.
- $[ASS4]$ - For the buckling and axial load analysis, the importance of the spherical caps was neglected as no source could be found online other than performing Finite Element Analysis. This shall be considered in the next design refinement.
- $[ASS5]$ - The lateral loading was not considered in the stress state as it is considered negligible compared to the axial one.
- $[ASS6]$ - Only a few failure modes are investigated in order to simplify the calculations. That is, failure by buckling and failure due to a stress state larger than yield stress.

The structure of the section follows Figure 2.3, presenting all relevant equations and methods. Throughout this text, mentions of the variables t_1, t_2, R and L are recurrent and those are therefore illustrated in Figure 2.4 for convenience.

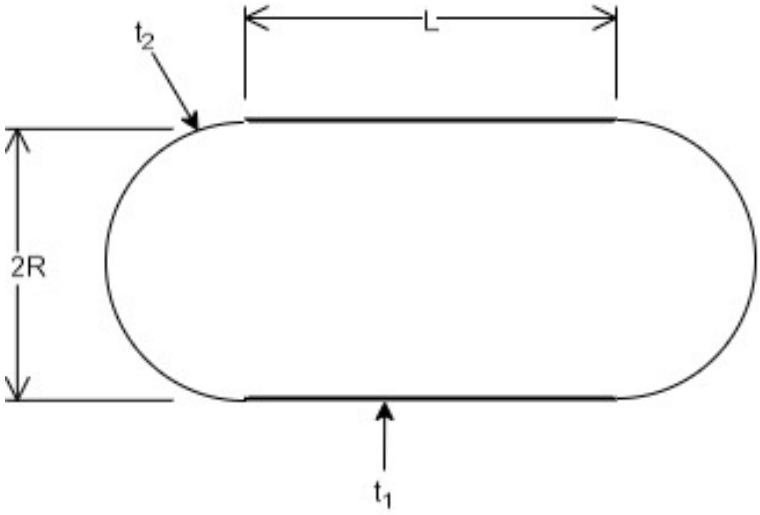

Figure 2.4: Main geometry of an oxidizer or fuel tank

As a way to check the procedure in the following, a first iteration using Aluminium 2024-T3 and an assumed value of the radius of 0.5 m. This is coupled with the values of 0.01 and 10 mm for the thickness of the spherical part. In this way, the results given numerically in this section cover the whole range of designs tested when it comes to the thickness of the spherical part.

2.3.1 Geometrical Properties

For each iteration, a value of R and t_2 are assumed and the rest of the structure's geometry is computed from this point. In this subsection, the methods to determine A, L and t_1 are discussed.

Thickness in Cylindrical Part

To calculate the thickness in the cylindrical part, a different approach needs to be taken. For the tank not to fail, there can be no discontinuities in the circular strain between the cylinder and the end caps [3], as this would result in very large stresses on the joints between those parts. This results in a ratio between the thicknesses of the sphere and the cylinder, from which the thickness of the cylindrical section follows. The strains of the two different sections in circumferential direction are given by Equations 2.4 and 2.5.

$$\epsilon_{cylinder} = \frac{pR}{t_1 E}\left(1 - \frac{v}{2}\right) \tag{2.4}$$

$$\epsilon_{sphere} = \frac{pR}{2t_2 E}(1 - v) \tag{2.5}$$

Equating these two strains results in the final ratio between the two thicknesses that needs to always be satisfied. This ratio is defined in Equation 2.6.

$$t_1 = \frac{2 - v}{1 - v} t_2 \tag{2.6}$$

Given the minimum and maximum values of the thickness of the spherical part of 0.01 mm and 10 mm respectively, and an assumed material of aluminium the thickness of the cylindrical part can be calculated as in Equation 2.7 and Equation 2.8.

$$t_{1,min} = \frac{2 - v_{aluminium}}{1 - v_{aluminium}} \cdot 0.01\ mm = 0.0249\ mm \tag{2.7}$$

$$t_{1,max} = \frac{2 - v_{aluminium}}{1 - v_{aluminium}} \cdot 10\ mm = 24.9\ mm \tag{2.8}$$

This shows that the thicknesses of the cylindrical part will need to be more than double that of the spherical part for most materials. The spherical shape is more efficient than that of a cylinder. From this insight it is expected that the final tanks will have a design that resembles a sphere, with only a short cylindrical section, as this will provide the lightest tank design.

Length and Cross Sectional Area

Using the assumed values of the radius and thickness of spherical caps as well as information about the total volume of fuel or oxidizer, the length of the cylindrical part is found from Equation 2.9. The numerical result from the assumed value of the radius is also given.

$$L = \frac{V - (4/3) \cdot \pi \cdot R^3}{\pi \cdot R^2} = 0.06545\ m \tag{2.9}$$

The cross sectional area in the cylindrical part is given by Equation 2.10. Note that the thin walled approximation $[ASS1]$ was not used here, since implementing the equation for non-thin walled structure was equally time-consuming.

$$A = \pi \left(R^2 - (R - t_1)^2\right) \tag{2.10}$$

For the minimum and maximum values of t_1 respectively, the cross sectional area is: $7.83 \cdot 10^{-5}\ m^2$ and $0.0783\ m^2$.

2.3.2 Mass of Attachments

A first estimate for the mass of the attachments of the fuel and oxidizer tanks can be obtained by scaling the mass found in WP4 [4] by the ratio of the resultants acting on both types of attachments. The forces used in WP4 to design the attachment are $F_{x_{wp4}} = 1643.2\ N$, $F_{y_{wp4}} = 1643.2\ N$, $F_{z_{wp4}} = 4929.5\ N$ and $F_1 = 950\ N$. F_y and F_1 act in the same direction, the resultant force $F_{res_{wp4}}$ is then determined as $5807\ N$. The total load through the propellant tanks together is assumed to be the total launch load, because the propellant tanks are to be part of the primary structure. The static axial and lateral load factors from WP4 [4] are $n_z = 5.5$ and $n_{lat} = 0.4$. Then the loads are calculated with Equation 2.11 and Equation 2.12. For illustration purposes the calculations of the first iteration using a spacecraft mass of 2304 kg determined in previous work packages is shown.

$$F_z = n_z \cdot g \cdot M = 5.5 \cdot 9.81 m/s^2 \cdot 2304\ kg = 124312\ N \tag{2.11}$$

$$F_{lat} = n_{lat} \cdot g \cdot M = 0.4 \cdot 9.81 m/s^2 \cdot 2304\ kg = 9041\ N \tag{2.12}$$

Once the total lateral and axial forces are known, the resultant force per attachment will be calculated in Equation 2.13.

$$F_{res_{attach}} = \frac{\sqrt{F_z^2 + F_{lat}^2}}{n_{attach}} = \frac{\sqrt{124312^2 + 9041^2}}{5} = 24930\ N \tag{2.13}$$

In order to scale the fuel tank attachment mass to the previously calculated solar panel attachment mass, first the force ratio was calculated and assumed to be equal to the mass ratio between the two attachment types. So the force ratio Q is calculated in Equation 2.14.

$$B = \frac{F_{res_{attach}}}{F_{res_{wp4}}} = \frac{24930\ N}{5807.3\ N} = 4.29 \tag{2.14}$$

Then, with Equation 2.15 the mass of a single attachment is calculated.

$$m_{attach} = n_{attach} \cdot B \cdot m_{attach_{wp4}} = 5 \cdot 4.29 \cdot 0.217\ kg = 4.66\ kg \tag{2.15}$$

The mass of this attachment system is quite a bit bigger than the previous one, as it needs to carry the loads through the tank, which is a structural member of the entire spacecraft. Then the total attachment mass will be added to the previous total spacecraft mass M (not containing any attachment) and the previous calculations will be re-done for that new mass. This iteration affects the attachment mass which carries through to the total spacecraft mass again. This cycle will continue until the total spacecraft mass converges. The detail of this part is also provided in the form of the Python code here:

```
        while diff > 10**(-5):
            M1 = M
            M_attachNew = massAttachments(M, m_attachwp4, n_attach)
            M += M_attachNew
            M -= M_attachOld
            M_attachOld = M_attachNew
            M2 = M
            diff = M2 - M1
```

Listing 2.1: Attachment mass convergence

The entirety of the Python code can be found in Appendix A.

2.3.3 Critical Stresses

In this subsection, the critical stresses due to the geometry and the material of the structure are discussed. Those critical stresses will be used to determine whether the structure would fail under a specific stress state.

Euler Buckling

Buckling of the propellant tanks is an important failure mode to consider due to the large axial compressive forces during launch. The critical stress due to Euler buckling can be calculated according to Equation 2.16 and the moment of inertia of the cross section is given from Equation 2.17.

$$\sigma_{cr} = \frac{\pi^2 EI}{AL^2} \tag{2.16}$$

$$I = \frac{\pi}{4}\left(R^4 - (R - t_1)^4\right) \tag{2.17}$$

Using the assumed values of 0.5 m for the radius and the maximum and minimum thicknesses t_1, the critical Euler buckling stress was determined to be 74.28 TPa for the largest t_1 and 21.05 TPa for the smallest. Therefore, the column buckling will probably not be a driving requirement.

Shell Buckling

Shell buckling is another type of failure mode that could occur in the cylindrical part of the structure. It is governed by Equation 2.18.

$$\sigma_{cr} = \left(1.983 - 0.983 \cdot e^{-23.14 \cdot Q}\right) k_{cr} \cdot \frac{\pi^2 E}{12(1 - v^2)} \cdot \left(\frac{t_1}{L}\right)^2 \tag{2.18}$$

In this equation, the values of Q and k_{cr} are left unknown and are given by Equations 2.19 and 2.20 respectively.

$$Q = \frac{p}{E}\left(\frac{R}{t_1}\right)^2 \tag{2.19}$$

$$k_{cr} = \lambda + \frac{12L^4}{\pi^4 R^2 t_1^2}(1 - v^2)\frac{1}{\lambda} \tag{2.20}$$

In Equation 2.20, the last unknown is λ that is depended on the number of half-waves along the length and circumference, along which the tank buckles. The value of λ should be selected to minimize Equation 2.20. Therefore, by setting $\frac{dk_{cr}}{d\lambda} = 0$, λ is found from Equation 2.21.

$$\lambda = +\sqrt{\frac{12 \cdot L^4 \cdot (1 - v^2))}{\pi^4 \cdot R^2 \cdot t_1^2}} \tag{2.21}$$

This means that Equation 2.18 can be used to determine the critical stress due to shell buckling in the structure. To continue the numerical computations, the shell buckling parameters are given in Table 2.2.

Table 2.2: Parameters values for shell buckling

Parameters	Minimum t_1	Maximum t_1
Q	13761.93	0.013761
λ	113.87	0.11387
k_{cr}	227.7	0.2277
σ_{cr}	4.42 MPa	2.82 GPa

Yield Stress

The yield stress of the material used will be checked in all parts of the structure. The stress state in the structure shall be smaller than this value in the entire structure to avoid any permanent deformation. As Aluminium is used for the numerical example carried out, the yield stress is 345 MPa for this first iteration.

2.3.4 Stresses Computations

In this subsection, the stresses present in the structure under the assumptions mentioned at the beginning of the section are determined.

Stress due to Internal Pressure

Given the radius and material of the tank, as well as the internal pressure at which the propellant shall be stored and the thickness of the spherical caps, the stresses in the pressure vessel can be calculated. There are two forms of stresses that the vessel is under, the longitudinal stress in the cylindrical part as well as the hoop stress in both the cylindrical and spherical parts. The hoop stress in the spherical caps is the largest and can be computed using Equation 2.22.

$$\sigma = \frac{p \cdot R}{t_2} \tag{2.22}$$

Following the numerical calculations, this stress is found to be 124.9 GPa and 125 MPa for the minimum and maximum thickness of the spherical caps respectively.

Axial Stress

The axial stress in the cylindrical part is found from the axial load applied on the structure. This comes from the fact that the fuel and oxidizer tanks are part of the integral structure and therefore experience the complete total load endured by the spacecraft. The longitudinal stress from the internal pressure shall be added as well to get the total stress in the structure. This is shown by Equation 2.23.

$$\sigma_{axial} = \frac{F_z}{A} + p \cdot \frac{R}{2 \cdot t_1} \tag{2.23}$$

This gives a value of the axial stress in the two cases considered of 26.65 GPa (for minimum t_1) and 26.72 MPa (for maximum t_1).

2.3.5 Failure Check

Finally, the failure is checked in the entire structure using the critical stresses discussed earlier. If the axial stress is larger than the most critical one (from buckling failures or yield), then the design is disregarded. That is also the case if the stress due to the internal pressure in the spherical caps is larger than the yield stress. The most appropriate design for a given material is then found from the list of all possible (non-failing) designs by choosing the one with the lowest mass. From this, the design for the smallest and largest t_2 are considered. The former fails due to yielding in the cylindrical and spherical part, an iteration is therefore necessary as the structure is obviously too thin. On the other side, the design with the largest t_2 is not failing but is way to heavy (103kg) as it is over-designed. It therefore also requires iterations. Note that the first design also fails due to shell buckling.

The same procedure is then repeated by a computer with different values. Once all possible designs were made and simulated for failure, the best once can be chosen with respect to mass.

2.4 Design selection

In this Section multiple designs are generated using the design procedure and the best design is selected. Since the material has not been selected and the design procedure provides the best design the main difference between the designs is the material used. In subsection 2.4.1 commonly used materials are studied and three materials are chosen to be compared in greater detail. In subsection 2.4.2 important properties of the designs are calculated using the design procedure and the results are summarized. Finally in subsection 2.4.3 the designs are compared, graded and the best design featuring a material is selected.

2.4.1 Materials

To find the best design some materials have to be chosen to be compared in detail. The materials that should be considered are ones used commonly in already existing propellant tank designs. Aerospace companies such as Moog Inc. and MT Aerospace use aluminum alloys, titanium alloys and stainless steel for their propellant tank designs [5] [6]. Comparing commonly used aluminum and titanium alloys used in the aerospace industry aluminum 2024 t3 and Ti-6Al-4V (grade 5) are chosen. Additionally, AISI type 304 stainless steel this chosen based on [7]. The materials and their properties are listed in Table 2.3.

Table 2.3: Materials and their properties

Property	**Aluminium** [1]	**Titanium** [2]	**Steel** [3]
E-modulus [GPa]	73.1	113.8	210
Yield strength [MPa]	345	880	215
Ultimate strength [MPa]	483	950	505
Poisson ratio [-]	0.33	0.342	0.28
Density $[g/cm^3]$	2.78	4.50	7.8
Cost [$/kg]	3.4	16.25	2.82

2.4.2 Designs

Using Python, three designs are made for the fuel tanks and three designs are made for the oxidizer tank. Each design features a different material. The script used can be found in Appendix A and was explained in section 2.3. The results for these designs are summarized in Table 2.4 and Table 2.10.

[1] Aluminum 2024-T3 [8] [9]

[2] Ti-6Al-4V (Grade 5), annealed [10][11]

[3] AISI Type 304 Stainless Steel [12] [13]

Table 2.4: Results of fuel tank designs

Geometry	**Aluminium**	**Titanium**	**Stainless Steel**
R [m]	0.505	0.505	0.505
L [m]	0.044	0.044	0.044
t_1 [mm]	9.15	3.63	14.05
t_2 [mm]	3.67	1.44	5.88
Mass [kg]	40.6	27.4	166.9
Material cost [$]	138.04	445.25	470.66

Table 2.5: Results of oxidizer tank designs

Geometry	**Aluminium**	**Titanium**	**Stainless Steel**
R [m]	0.467	0.467	0.467
L [m]	0.045	0.045	0.045
t_1 [mm]	8.45	3.35	12.97
t_2 [mm]	3.39	1.33	4.50
Mass [kg]	33.2	22.7	133.7
Material cost [$]	112.90	368.44	377.00

In Table 2.4 and Table 2.10 the material cost of the tank designs are given, however this does not tell the full story of the costs as the manufacturing shall also be taken into account. The exact costs cannot really be estimated with some standard procedures. Using [14] it can be concluded that steel is cheaper in terms of the material cost per kilogram and in terms of manufacturing compared to aluminium. Next to that for from [15] it can be concluded that titanium is the most expensive material to use. The manufacturing costs are really high compared to aluminium and steel.

It is also seen from both Tables 2.4 and 2.10 that the design with the smallest mass corresponds to the same ratio of the length and the radius which is 11.477 for the fuel tank and 10.377 for the oxidizer tank. This shows that those fineness ratios give the lowest mass for both designs and changing the volume required would result in different dimensions for the same fineness ratio probably.

2.4.3 Material Trade Off

To find the best suited material for the tanks the designs composed are compared and a trade-off is made. In Table 2.6 criteria, their weights and a rationale for the criteria are given.

Table 2.6: Trade off criteria

Criteria	Weight	Rationale
Mass	70%	The mass of the tanks are the most important. It directly influences the dry mass of the spacecraft and thus the amount of propellant needed. This has a large effect for the costs.
Cost	30%	The cost of the propellant tanks is less important than the mass of the propellant tanks as its expected cost a lot less. However for some materials this may not be the case, so the costs of manufacturing should be investigated
Degradation	-	The material of the tank will be subjected to a harmful environment and the material may be able to degrade. It is important to take this into account as the mission will take seven to twelve years and the material can be weakened significantly. This could seriously endanger the mission, therefore a special kind of weight is assigned to this criteria. If the material is able to degrade due to the environment it may not be chosen.

Now the criteria and their weights have been established the designs featuring the materials have to be graded. The trade off will be done based on a score from 1 to 10 with 1 being to lowest score and 10 the highest score. In the end a weighted average is taken and a material can be chosen. The grades and the weighted average of the designs are found in Table 2.7.

Table 2.7: Scores of the Trade Off

Criteria	Aluminium	Titanium	Stainless Steel
Mass (70%)	6	8	3
Cost (30%)	6	3	8
Degradable	Yes/no [4]	No	No
Total Weighted Score	6.0	6.5	4.5

From Table 2.7 it becomes clear that Titanium Ti-6Al-4V is best suited for the final design, it has the highest weighted average and does not degrade due to corrosion. An in depth reasoning for the assigned scores can be found in the following subsections.

Mass

Titanium is found to be the lightest design and therefore will receive the highest score, however other materials that are not considered may be lighter so titanium will receive an 8 as score. Next to this is the aluminum design, it is not light but also not a heavy design, therefore 6 is chosen as its score. Finally is the steel design, it is simply terrible in terms of mass. The design is more than 6 times as heavy as the titanium design however there are without a doubt even worse materials to choose also and a 3 is assigned as score.

Costs

Aluminum wins in terms of material costs, however as mentioned earlier the manufacturing costs of steel are lower and titanium is a lot more expensive. Because the design is quite large the manufacturing costs are assumed to outweigh the material costs and the ranking from subsection 2.4.2 is followed. Titanium is very expensive and receives a 3, Aluminum is intermediate in terms of manufacturing costs and is scored a 6 and finally stainless steel is the cheapest in terms of manufacturing and receives an 8.

[4] Aluminum 2024 can corrode when it is used for the oxidizer tank, but cannot when used for the fuel tank

Degradation

To make sure that a material is chosen that does not degrade the materials should not corrode when the fuel or oxidizer is present in the tank.
Hydrazine has been selected as the fuel. This is a highly toxic fuel that is compatible with Aluminum 2024, Titanium Ti-6Al-4V and 304 stainless steel according [16]. Therefore all materials may be considered for the fuel tank.
Nitrogen tetroxide is a commonly used oxidizer for propellants and has also been selected as the oxidizer of this mission. A side affect of the oxidizer is that it has serious corrosion problems. When it is contaminated with water it becomes corrosive to aluminium, titanium and 304 stainless steel. This is a problem because of the high affinity for water and the fact that it becomes corrosive at a contamination of 0.2%. The corrosion can be prevented using an inhibitor. In a report [17] the best inhibitor to stop the corrosion is to be ammonium fluorosulfate (NH_4SO_3F). It however only protects titanium and 304 stainless steel. There is no inhibitor found that protects Aluminium from corrosion, therefore it will be a risk to the mission to select any aluminum alloy for the oxidizer tank design.

2.5 Final Design

In this section the final design will be presented. From iteration a few designs were generated, in the material trade off the designs are compared. In section 2.5.3 the important characteristics of the final design are presented. In section 2.5.4

2.5.1 Comparison to Previous Design

In WP2 [1] the tank design was only developed in order to withstand the pressure loads from the propellant and for weight efficiency purposes the design of the tank was chosen to be a sphere (since its the most weight efficient shape for propellant tanks [18]). Furthermore, the configuration of the tanks was determined to be 2 fuel tanks and 1 oxidizer tank. This configuration follows a similar configuration used by the Juno orbiter [1].

On the other hand, the current design includes many more realistic failure modes that the tank is tested for, this is done by designing for stress caused by pressure and launch loads. Additionally, the following failure modes are taken into account:

- Euler column buckling
- Shell buckling

Given that the re-iterated design of the tank now has much more restrictions due to the constraints set by the failure modes mentioned in the list above, the design of the current tanks will result in having different dimensions and characteristics compared to the previous design in WP2. For the sake of comparison, instead of having 3 tanks as in the previous design, the number is now reduced to 2 (one being an oxidizer tank and the other being a fuel tank) using the same procedure mentioned in WP2 [1] and thus giving the following tables represented by Table 2.9 and Table 2.8 which presents the comparison between the current and previous designs.

In addition to this, the current design will give a slightly better estimate of what the tank mass is, compared to the one calculated in work package 2, because of the constraints imposed on the design. In order to have the most accurate result the following procedure should be followed: with every iteration in the python code the change of mass compared to the previous iteration should be taken into account as a change in structural mass, then the change in structural mass will give rise to a new Delta V requirement which increases/decreases the amount of propellant mass needed. Then, the new propellant mass is used to produce new tank dimensions with different masses which once again causes a change in the total structural mass. This procedure should

be repeated until it converges and reaches a point where appropriate values for the mass of the tanks and the mass of the propellant are generated, thus giving a much more accurate result for the total structural mass of the spacecraft. The procedure is repeated further for different starting values of R,t and L, to find the design for the tank which gives the best estimate on the structural mass of the spacecraft.

Table 2.8: Current tank design

	Oxidizer tank	**Fuel tank**
Full length	0.979 m	1.054 m
R	0.467 m	0.505 m
t_1	3.35 mm	3.63 mm
t_2	1.33 mm	1.44 mm
Mass	22.7 kg	27.4 kg
Number of attachments	5	5

Table 2.9: WP2 tank design

	Oxidizer tank	**Fuel tank**
Full length	0.95 m	1.0317 m
R	0.475m	0.516 m
t	1.52 mm	1.64 mm
Mass	19.5kg	24.7
Number of attachments	1	1

2.5.2 Additional Considerations

In this report, instead of using CNT based composite as the material for the primary structure, Aluminium 2024-T3 has been used instead in order to give a more reasonable thickness of 2.55 mm using the method used in [1] and E-modulus of 70 GPa, however the mass that is added to the structural mass as a result of changing the material has not been added since changing the mass would change the delta v requirement and thus the total propellant mass, then further iteration will be done in order to get the final mass of the spacecraft, therefore in this report any additional mass as a result of changing the primary structure material is ignored, due to time constraints.

2.5.3 Summary final design

In subsection 2.4.3 a material trade off was conducted and it is found that the oxidizer and fuel tank design using titanium as material is best suited for the design goals. The designs are summarized in Table 2.10.

Table 2.10: Final oxidizer and fuel tank designs

Geometry	**Fuel tank**	**Oxidizer tank**
R [m]	0.505	0.467
L [m]	0.044	0.045
t_1 [mm]	3.63	3.35
t_2 [mm]	1.44	1.33
Mass	27.4	22.7
Material cost [$]	445.25	368.44

2.5.4 Final design models

In figure 2.5 a model of the fuel tank system can be seen. In figure 2.6 a model of the fuel tank configured in the JUNO spacecraft can be seen.

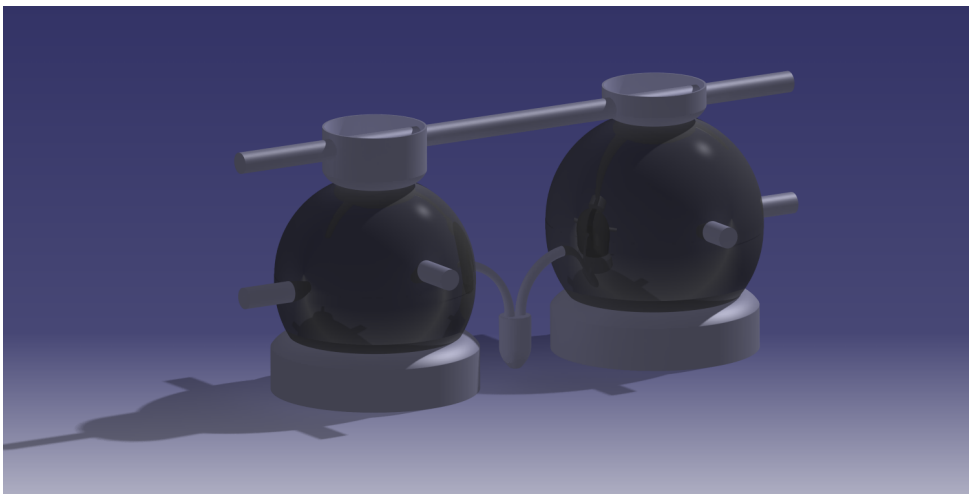

Figure 2.5: CATIA model of the fuel tank

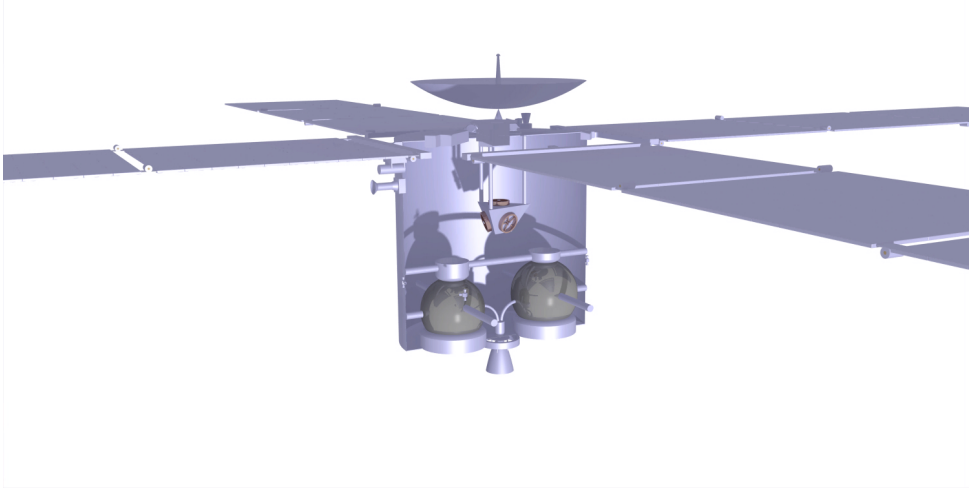

Figure 2.6: CATIA model of fuel tank design inside the JUNO spacecraft

Dynamic study 3

This chapter shows the process of performing a dynamic study on the spacecraft. In Section 3.1 the entire spacecraft is analyzed as a single degree of freedom system to find its natural frequency. In Section 3.2 the natural frequencies of the tanks are determined. Additionally, in Section 3.3 the structure will be modeled as a two degrees of freedom system, where the spacecraft is connected to the launch vehicle using a connection of a certain stiffness, and the previously designed fuel tank to the spacecraft with another stiffness. Finally, in Section 3.5, the single degree of freedom system will be analyzed in the case of a forcing function, as is the case on the launch vehicle.

Assumptions made during the chapter

- $[ASS7]$ - Mass of each component (primary structure or tank) is assumed to be concentrated at the end of the structure.
- $[ASS8]$ - The axial stiffness K_{Axial} is assumed to be the axial stiffness of a rod with the mass concentrated at its end (from [19]).
- $[ASS9]$ - $K_{Lateral}$ is assumed to be the later stiffness of a cantilever beam with the mass concentrated at its end (from [19]).
- $[ASS10]$ - The cross-sectional area of the tanks is approximated to be the cross-sectional area of the cylindrical part of the tank in order to simplify the calculations.
- $[ASS11]$ - When taking the cross-sectional areas of the propellant tanks, only the cross-sectional area of the cylindrical part is used in the calculations as an approximation (since cross sectional area will be changing through out the tank). Additionally since the thickness of the cylindrical and spherical parts of the tanks are different an average thickness is used when computing the cross-sectional area. Although this is a non-conservative approach the cross-sectional area that is used will not differ by a great amount to the average cross-sectional area of the whole tank

3.1 1-Degree of Freedom

In order to make sure that the spacecraft does not resonate during launch, it is required its natural frequency more than that of what the launcher specifies. This is done by modeling the spacecraft as a mass attached to a spring with a stiffness of k as 3.1 portrays.

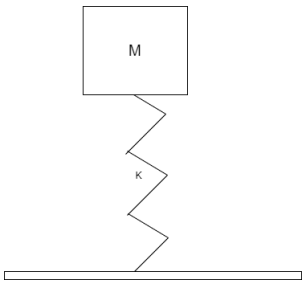

Figure 3.1: Modelling of the tank as a spring system

Figure 3.1 present the spring system that is used to approximate the natural frequencies of the system. From these, two spring constants are estimated, the first being the axial direction using Equation 3.2 and the second being for the lateral direction with Equation 3.3 (From [ASS8] and [ASS9] in subsubsection 3)[18]. Equation 3.1 is used the compute the natural frequency.

$$f_n = \frac{1}{2\pi}\sqrt{\frac{k}{M}} \quad (3.1) \qquad K_{Axial} = \frac{EA}{L} \quad (3.2) \qquad K_{Lateral} = \frac{3EI}{L^3} \quad (3.3)$$

After some manipulations, Equations 3.4 and 3.5 can be obtained for the lateral and axial natural frequency respectively.

$$f_n = \frac{1}{2\pi}\sqrt{\frac{3E\pi r^3 t}{ML_p^3}} \quad (3.4)$$

$$= \frac{1}{2\pi}\sqrt{\frac{3 \cdot 70 \cdot \pi \cdot 1.5^3 \cdot 2.55 \cdot 10^{-3} \cdot 10^9}{2308.26 \cdot 3^3}}$$

$$= 48.038\ Hz$$

$$f_n = \frac{1}{2\pi}\sqrt{\frac{E\pi Dt}{L_p M}} \quad (3.5)$$

$$= \frac{1}{2\pi}\sqrt{\frac{\pi \cdot 70 \cdot 3 \cdot 2.55 \cdot 10^{-3} \cdot 10^9}{3 \cdot 2308.26}}$$

$$= 78.44\ Hz$$

Based on 3.5 and 3.4 it is clear that the design of the spacecraft has a natural frequency that is sufficiently larger than the natural frequency limitations set by the launcher which are 8 Hz and 15 Hz in the lateral and longitudinal direction respectively.

3.2 Tank Natural Frequency

The same analysis that has been performed in the previous section can be repeated for the tank that will be attached to the structure of the spacecraft. The tank is composed of two half spheres and a small cylinder in the middle as it is showed in Figure 3.2. To calculate the natural frequency, the axial stiffness is determined using Equation 3.6(based on [ASS8]) with the area is approximated by a thin-walled cylinder with a thickness being the average of the both t_1 and t_2. ([ASS11]). The E-modulus of Titanium of 134 GPa is used

$$K_{axial} = \frac{EA}{L} = 9.398 \cdot 10^8\ N/m \quad (3.6)$$

The natural frequency in the longitudinal direction is then computed using Equation 3.1 with $k = K_{axial}$. This gives 198.6 Hz which is pretty high, due to the high E-modulus of the titanium the tank is made of.

The same analysis can be repeated for the oxidizer tank, which has the same shape as the fuel tank but it is slightly smaller in volume. The same assumptions are used and after plugging in the values in Equation 3.6 an axial stiffness K_{axial} of $1.0246 \cdot 10^9 N/m$ is found. This results in a natural frequency of 216.23 Hz.

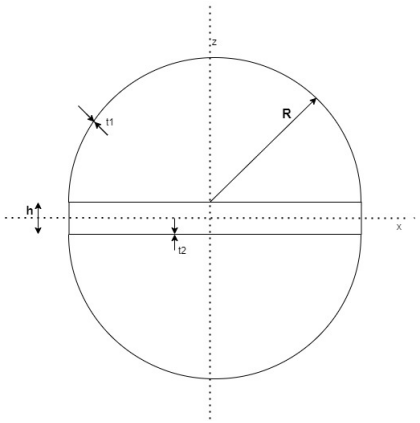

Figure 3.2: Cross section of the tank

3.3 2-DOF system for the entire spacecraft

In this section the spacecraft system will be analysed as a system of two degrees of freedom system by attaching the mass of the spacecraft to another mass using a shaft of stiffness k_2, whilst the spacecraft is attached to the launcher by a shaft of stiffness k_1. The discretised system is shown in Figure 3.3.

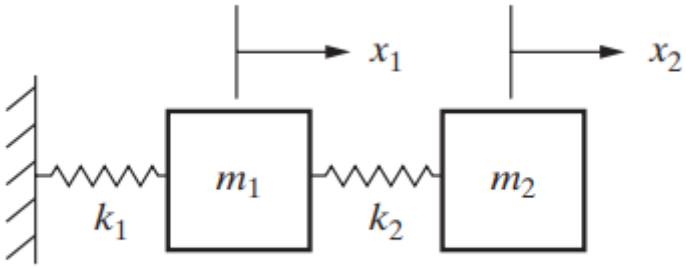

Figure 3.3: 2-DOF system

The FBD of the two masses in the system is shown in Figure 3.4 and the system of equations of motions 3.7 follow directly from them.

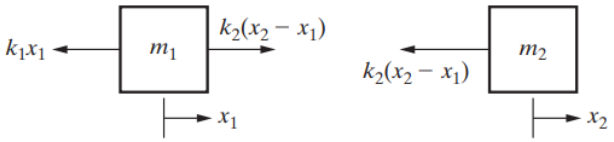

$$\begin{cases} m_1\ddot{x_1} = -k_1x_1 + k_2(x_2 - x_1) \\ m_2\ddot{x_2} = -k_2(x_2 - x_1) \end{cases} \tag{3.7}$$

Figure 3.4: Free body diagram of system

The system of differential equations 3.7 should be solved to describe fully the motion of the structure. To do that, the initial conditions of the system should be identified. The system is at rest before launch and therefore, the initial conditions are assumed to be Equation 3.8:

$$\begin{cases} x_1 = 0 \ \wedge \ x_2 = 0 \\ \dot{x_1} = 0 \ \wedge \ \dot{x_2} = 0 \end{cases} \tag{3.8}$$

3.4 Solving the 2-DOF system of equations

In order to solve the system Equation 3.7, it is converted to matrices. Note that the calculations shown in this section will be repeated twice in order to account for the spacecraft connecting to the fuel tank and also the oxidizer tank. Equation 3.7 can be rewritten as Equation 3.9.

$$M\ddot{x} = \begin{bmatrix} m_1\ddot{x_1} \\ m_2\ddot{x_2} \end{bmatrix} \qquad Kx = \begin{bmatrix} k_1 + k_2 & -k_2 \\ -k_2 & k_2 \end{bmatrix} \cdot \begin{bmatrix} x_1 \\ x_2 \end{bmatrix} \qquad M\ddot{x} + Kx = 0 \tag{3.9}$$

In order to solve this matrix equation, the method outlined in [19] is used. First, it is assumed that ue^{iwt} is a solution to the differential equation and therefore a characteristic equation could be computed as follows using the fact that $e^{iwt} \neq 0$ and $u = \begin{bmatrix} u_1 \\ u_2 \end{bmatrix}$

$$(-\omega^2 M + K) \cdot ue^{iwt} \equiv (-\omega^2 M + K) \cdot u = 0$$

$$det(-\omega^2 M + K) = 0 \equiv \begin{vmatrix} -\omega^2 m_1 + k_1 + k_2 & -k_2 \\ -k_2 & -\omega^2 m_2 + k_2 \end{vmatrix} = 0$$
$$\equiv m_1 m_2 \omega^4 - (m_1 k_2 + m_2 k_1 + m_2 k_2)\omega^2 + k_1 k_2 = 0 \tag{3.10}$$

Therefore in order to solve Equation 3.10 and find a value of ω. The values of k_1 and k_2 are used from Equations 3.2 and 3.6 in addition to the mass[1] of the spacecraft and the fuel tank to give the characteristic equation Equation 3.11.

$$1028464\omega^4 - 2.5075 \cdot 10^{12}\omega^2 + 5.27 \cdot 10^{17} = 0 \tag{3.11}$$

The smallest (real) solution of the equations is used.

$$\omega^2 = 232303\ rad^2/s^{-2} \qquad f_o = \frac{\omega}{2\pi} = 76.7\ Hz \tag{3.12}$$

Furthermore, Equation 3.10 is used once again to compute the natural frequency of the system however this time the calculations are done for the fuel tank being attached instead of the oxidizer tank to give the following equation.

$$973179\omega^4 - 2.676 \cdot 10^{12}\omega^2 + 5.746 \cdot 10^{17} = 0 \tag{3.13}$$

$$\omega^2 = 234767\ rad^2/s^{-2} \qquad f_f = \frac{\omega}{2\pi} = 77.1\ Hz \tag{3.14}$$

Given that the natural frequencies that were acquired in sections 3.1 and 3.2 are less than the acquired frequencies in this section, it is more reasonable to size for the 2 degree of freedom system instead of 1 degree of freedom, however in this case the minimum required natural frequency according to the Atlas V launch manual is 15 Hz in the longitudinal direction, which means that the current design has surpassed the constraint that is set by the launcher manual [20].

3.5 Forced Vibration

During launch, the launch vehicle also imposes dynamical loads to the spacecraft besides the earlier considered static loads. In order to approximate this situation the propellant tanks will be vibrated by a sinusoidal varying force with the amplitude equal to the axial dynamic loading of the launch vehicle. So this force is added to the axial spring system from Section 3.2. The resulting equation is:

$$\ddot{x} + \omega^2 x = F cos(\omega_f t) \tag{3.15}$$

In Equation 3.15 F is the dynamic force of the spacecraft in axial direction and ω_f is the frequency of the dynamic load. In order to solve the equation the Laplace Transform of both sides is taken resulting in:

$$s^2\mathcal{L}\{x\} - sx(0) - \dot{x}(0) + \omega^2\mathcal{L}\{x\} = F\frac{s}{s^2 + \omega_f^2} \tag{3.16}$$

Similar to section 3.3 the following boundary assumptions are used:

$$\begin{cases} x(0) = 0 \\ \dot{x}(0) = 0 \end{cases}$$

Now, Equation 3.16 can be reduced to Equation 3.17:

$$\mathcal{L}\{x\} = F\frac{s}{(s^2 + \omega_f^2)(s^2 + \omega_f^2)} = \frac{F}{\omega_f^2 - \omega^2}\left(\frac{s}{s^2 + \omega^2} - \frac{s}{s^2 + \omega_f^2}\right) \tag{3.17}$$

[1] mass of spacecraft + fuel used was 1705.085kg and mass of oxidizer is 603.175

[2] in this calculation the masses used are 1753.16kg for the spacecraft + oxidizer and 555.1kg for the fuel mass

So the solution will be:

$$x(t) = \frac{F}{\omega_f^2 - \omega^2} \left(cos(\omega t) - cos(\omega_f t)\right) \tag{3.18}$$

Note that in Equation 3.18 $\omega_f \neq \omega$ as otherwise division by zero would occur (resonance). In order to get the final solution, the parameters F, ω and ω_f need to be put into Equation 3.18. As there are two tanks, two expressions will be made, one for each tank. According to WP2 [1] the maximum axial dynamic load is $2g$ which means that $F = 2gM$. As both tanks are similar, it is assumed that each tank carries half the load. So then $F = gM$ for each tank. $f = 100\ Hz$ from the project manual. So with $\omega = 2\pi f$, the forced angular frequency is $\omega_f = 200\pi\ rad/s$ and with the natural frequencies of the oxidiser and fuel tank from section 3.2 the angular natural frequencies can be calculated as follows:

1. $\omega_{ox} = 2\pi \cdot 198.6\ Hz = 1248\ rad/s$
2. $\omega_{fuel} = 2\pi \cdot 216.23\ Hz = 1359\ rad/s$

Now all parameters are known, the deflections of both tanks with respect to time can be modelled. This is done in python. First the deflection vs time graph of the oxidiser tank is given (Fig. 3.5).

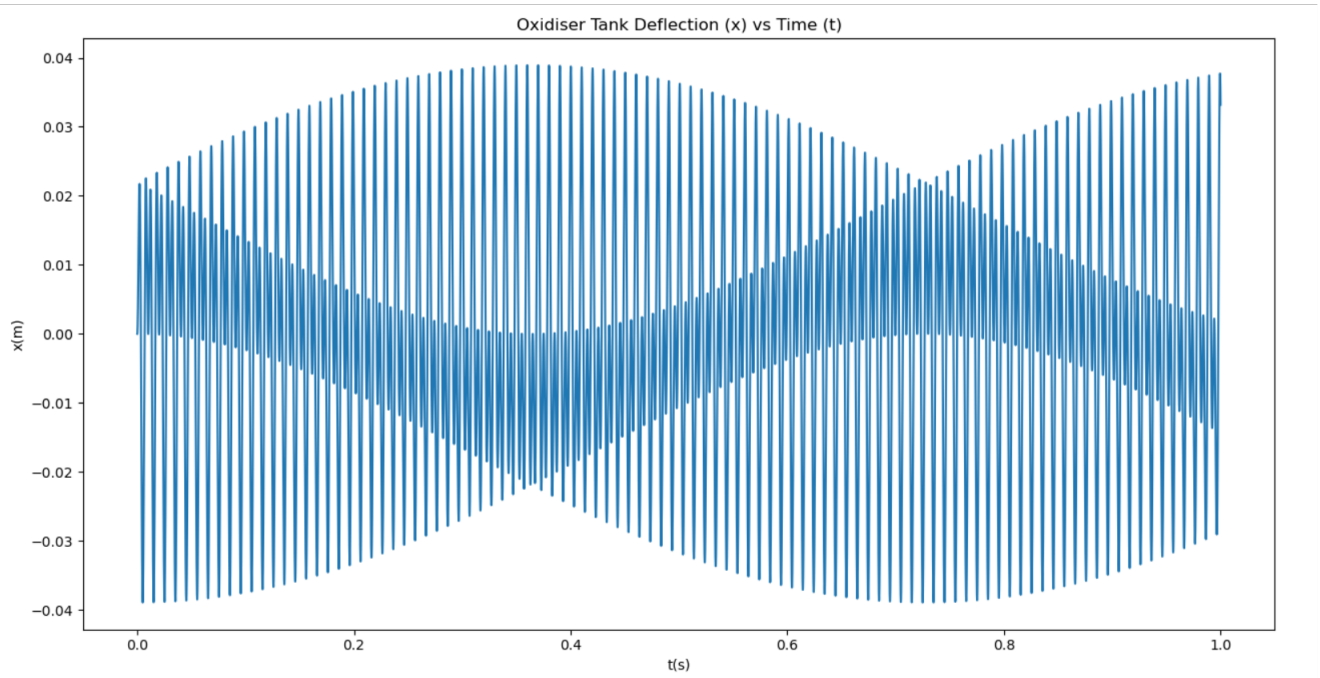

Figure 3.5: Deflection vs time graph of the oxidiser tank

Now the deflection vs time chart of the fuel tank is given in Fig. 3.6.

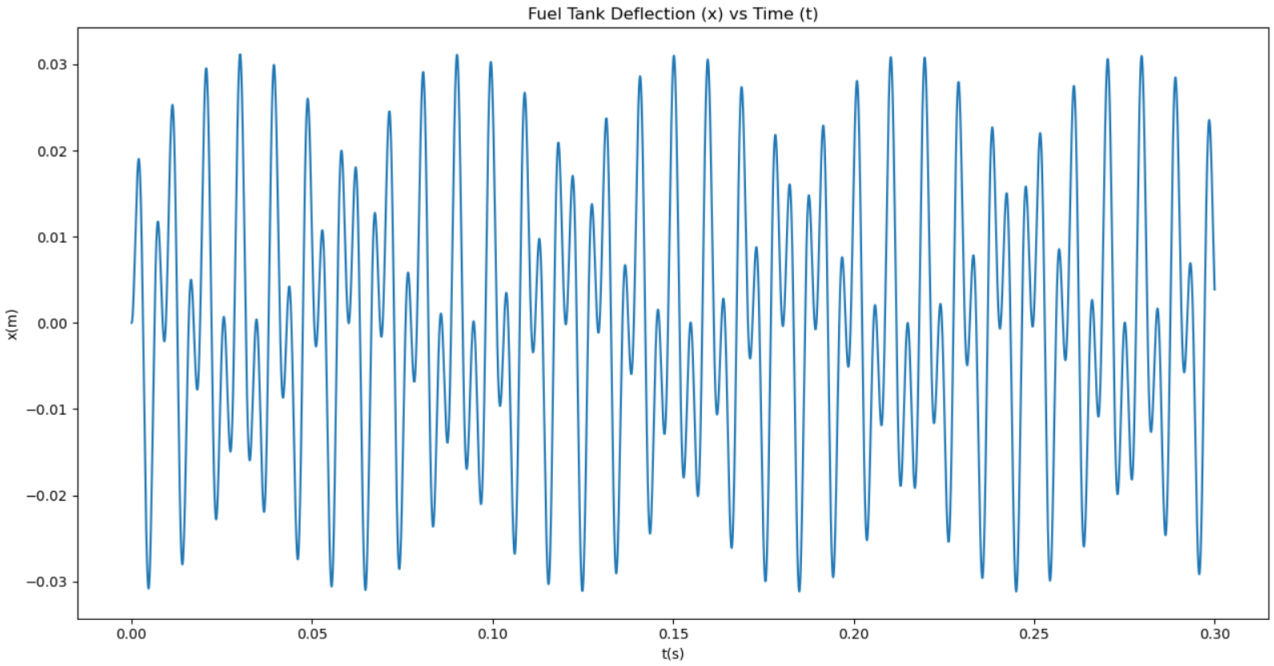

Figure 3.6: Deflection vs time graph of the fuel tank

As can be seen from Fig. 3.5 and Fig. 3.6, the variation of the amplitude with respect to time is less for the oxidiser tank than for the fuel tank. This is due to the natural frequency of the oxidiser tank being closer to a multiple of the forcing frequency ($2 \cdot 100\ Hz$) than the one of the fuel tank.

In order to get the maximum amplitude as a function of the forced frequency, first an expression of the amplitude has to be found. The maximum deflection occurs when $cos(\omega t) - cos(\omega_f t)$ is maximum and this maximum value will be 2. So the expression of the amplitude as a function of forcing frequency will be as in Equation 3.19.

$$A(\omega_f) = \left| \frac{2F}{\omega_f^2 - \omega^2} \right| \tag{3.19}$$

This relation will be plotted for both the oxidiser tank (Fig. 3.7) and the fuel tank (Fig. 3.8).

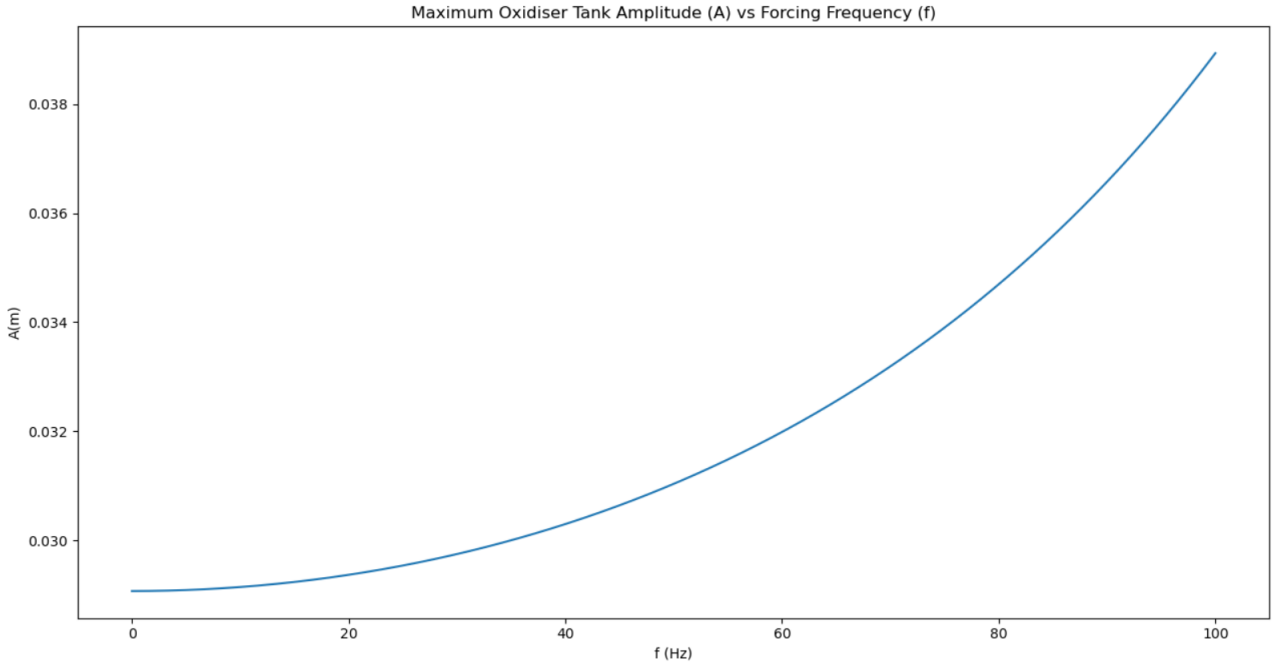

Figure 3.7: maximum amplitude vs forcing frequency graph of the oxidiser tank

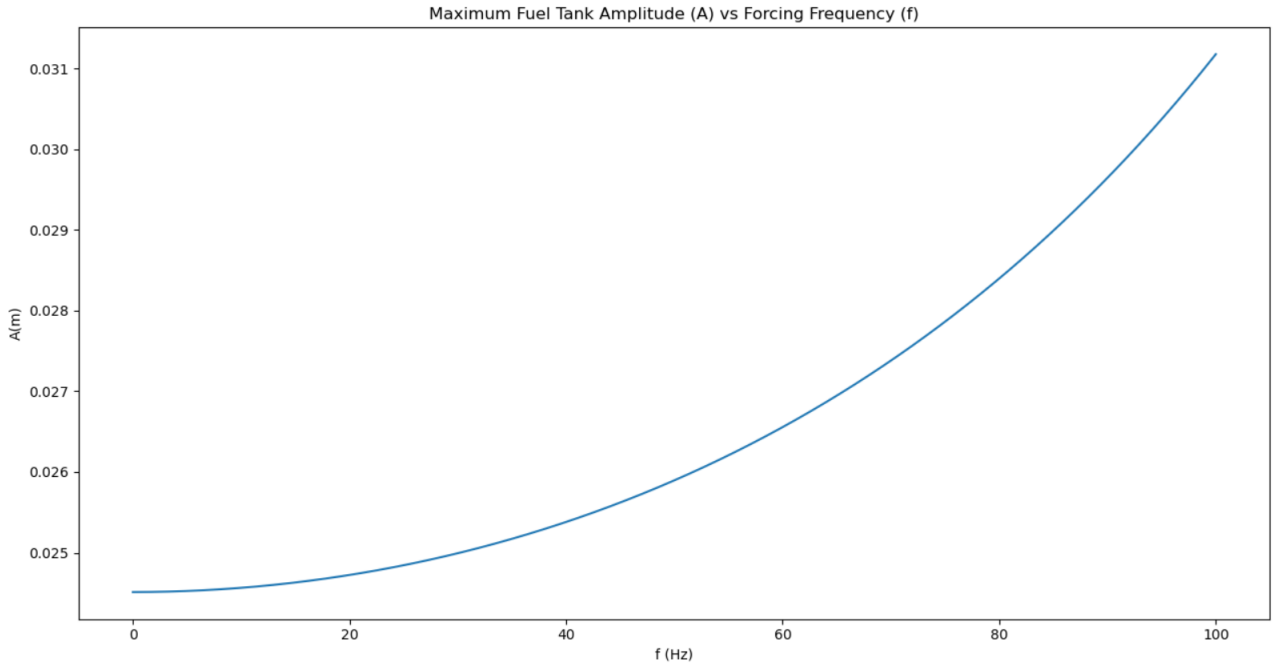

Figure 3.8: Maximum amplitude vs forcing frequency graph of the fuel tank

As the natural frequencies of both tanks are significantly higher than the given range of forcing frequencies, the maximum amplitude of the vibrations in the tanks will only increase slightly over the interval of 0 Hz to 100 Hz. In order to illustrate this better consider Fig. 3.9 in which the amplitude versus forcing frequency graph of the oxidiser tank is extended to 300 Hz.
Furthermore, from the graphs it can be seen that fuel tank will have a lower maximum amplitude than the oxidiser tank at a given forcing frequency. This makes sense, because the natural frequency of the fuel tank is higher than that of the oxidiser tank according to Section 3.2 and the closer the forcing frequency is to the natural frequency the bigger the maximum amplitude will get.

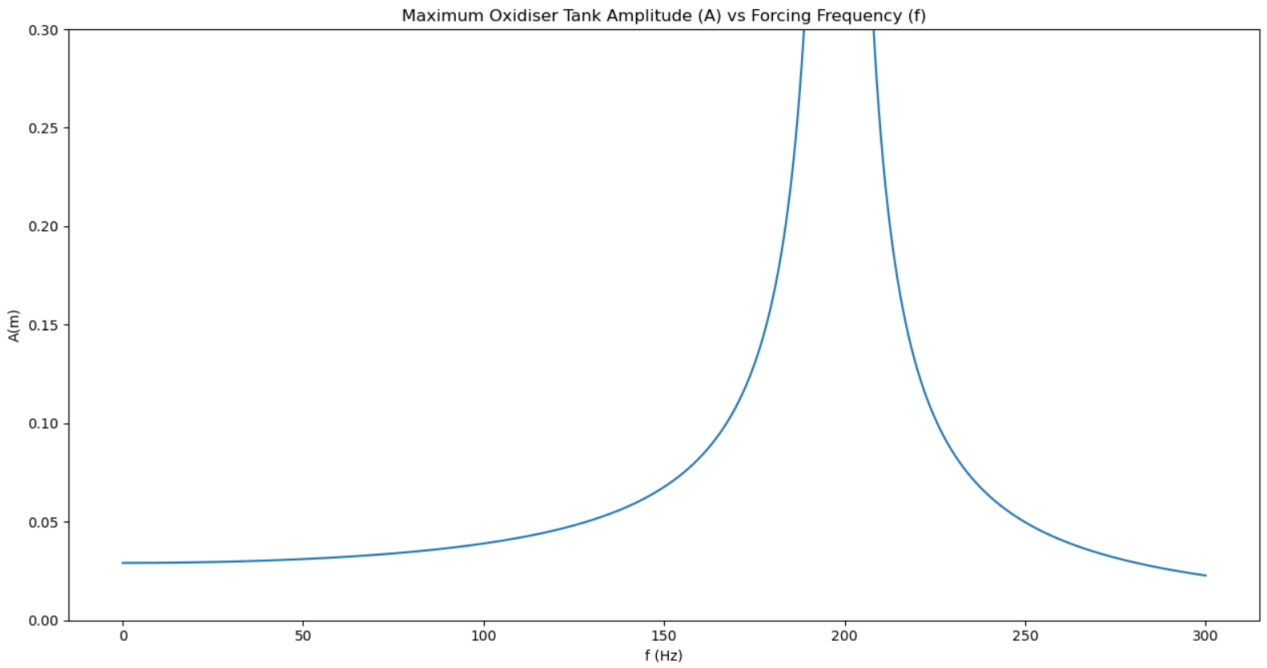

Figure 3.9: Maximum amplitude vs forcing frequency graph of the oxidiser tank between 0 Hz and 300 Hz

3.6 Conclusion

So from the previous analyses it is found that the spacecraft will withstand the dynamic loads imposed by the launch vehicle. In Section 3.1 it is found that the natural frequencies of the spacecraft are above the required frequencies of the payload in the launch vehicle. Also when the spacecraft is analysed as a system with two degrees of freedom, in Section 3.3, the natural frequency came out to be higher than the required minimum natural frequency. Finally, in Section 3.5 it was found that the forced testing frequencies were far from the natural frequencies of the tank causing relatively low response of the tanks. So no resonance will occur in the spacecraft.
However, in further design stages this analysis needs to be done in more detail. For example, the masses of the attachments are neglected, but these can certainly play a role in failure due to dynamic loads. So for a more accurate representation of the spacecraft more degrees of freedom may be needed.

Potential Damage Due to Meteoroids and Orbital Debris 4

While the solar system is usually thought of as a vast expanse of empty space with only a few planets around the Sun, there exist many particles of very low mass and volume. However, due to the extremely high velocities they usually carry large amounts of energy. Therefore, an impact with a spacecraft can be devastating for its mission. First, in section 4.1, the relevant particles to be analyzed are defined. The penetration depths are calculated in section 4.2 and the damages following the impacts are discussed in section 4.3.

4.1 Relevant types of objects

Since the spacecraft will be in earth's vicinity for only a short time after launch, human made orbital debris will not be considered as that is contained relatively close to earth. Thus only micrometeoroids that are present throughout the entirety of the solar system are considered. These usually have an average density of around 2.5 to 3 $\frac{g}{cm^3}$ [21]. The amount of micrometeoroids is not uniformly distributed over the different sizes. The amount of MM impacts is relatively uniform for sizes lower than $1.26 \cdot 10^{-8}$ g and then decreases for increasing sizes, eventually going to near zero around $3.39 \cdot 10^{2}$ g [22]. Thus the smaller particle size to be analyzed is the largest particle in the region of uniform amounts of impacts with a mass of $1.26 \cdot 10^{-8}$ g, as it has the same probability to occur as smaller ones but greater effect on the spacecraft. For the larger particle to be analyzed the particle size that has 0.05 impacts over the entire mission life considering the preliminary spacecraft cross sectional area of only the bus will be selected. This results in a particle of around $8.04 \cdot 10^{-4}$ g to be analyzed as the upper end. For all of the analyzed particles a density of 3 $\frac{g}{cm^3}$ will be assumed.

4.2 Penetration depth of particles

The particles will penetrate the surface they impact to a certain depth. It can be determined using Equation 4.1.

$$t = K m_p^{0.352} v_p^{0.875} \rho_p^{0.167} \tag{4.1}$$

t is the thickness to avoid penetration in cm, K is a material coefficient, for which 0.7 is a conservative estimation. The mass of the impacting particle is m_p in g and v_p is the impact velocity in $\frac{km}{s}$. ρ_p is the density of the particle given in $\frac{g}{cm^3}$, which in this case will be the average density found in the previous section. Using the previously selected particle sizes of $1.26 \cdot 10^{-8}$ g and $8.04 \cdot 10^{-4}$ g as well as the average velocity 17 $\frac{km}{s}$ [22] of micrometeoroids results in thicknesses of 0.166 mm and 8.168 mm to prevent penetration. The smaller particle size thus does not penetrate the wall with the current wall design, while the larger one will.

4.3 Damage produced

As previously determined the wall thickness of the JUICE Orbiter will be $0.78\ mm$ [1], thus stopping the smaller particles with ease. The largest particle size that the previously determined wall thickness can stop is around $1.055 \cdot 10^{-6}$ g, corresponding to 1.08 impacts of that particle size over the entire mission [21]. Thus it is very probable that larger particles than can be stopped will impact the spacecraft. The larger particle size with

a lower probability of impact poses an even larger problem. The wall thickness required to prevent penetration from a particle of that size is not attainable, as it would require wall thicknesses that increase the mass of the structures more than is feasible. Thus some alternative mitigation measures should be implemented, such as protective shielding such as a Whipple shield [23]. Additionally smaller impacts that do not penetrate the shell can still cause damage by providing points at which cracks can form that grow over time, eventually leading to failure. This mode of failure however can be neglected, since the structure design is driven by the launch loads. These loads only occur once during the beginning of the mission. Thus once in orbit and on its mission the loads will be minimal compared to launch, and only apply during maneuvers and attitude corrections. These loads do not apply often and are small in magnitude. These factors make crack formation negligible and therefore do not need to be considered further. Thus further research into micrometeoroid protection is warranted.

Conclusion and Recommendations 5

The aim of this report is to make a detailed fuel tank design and finds its dynamic loading during launch. These results were obtained by multiple steps given by the Work Package 5 reader.

Firstly, it was important to decide on the design of the propulsion system inside the spacecraft bus. This was realized by a few calculations and a rough sketch of the design. Moreover, the team slightly changed their propulsion design from Work Package 3, namely that it has one oxidizer and one fuel tank, and that the tanks are cylindrical instead of spherical. Additionally, in order to find the launch loads, material properties are highly needed for calculations and later-on iterations. Therefore, a material trade-off has been constructed with three main criteria, of which: mass, costs and degradation. Using these criteria, Titanium was found to be the best material for both the propulsion tanks. Furthermore, the launch were needed in order to check if the design would hold for the undergoing loads. This was found by calculating critical stresses, such as Euler buckling, shell buckling and stress due to the internal pressure of the tanks. With the rough design, material and launch loads; iteration was able to start and form the final design of the propulsion system. The final design is summarized in Table 5.1

Table 5.1: Tank designs

Geometry	**Oxidizer tank**	**Fuel tank**
R [m]	0.467	0.505
L [m]	0.045	0.044
t_1 [mm]	3.35	3.63
t_2 [mm]	1.33	1.44
Mass	22.7	27.4
Material	Titanium	Titanium
Material cost [$]	368.44	445.25

In the dynamic studies section the spacecraft has been modelled in different ways in order to make sure that the natural frequency of the spacecraft does not resonate with the minimum frequency set by the launcher, this is done by first analysing the whole spacecraft and getting the natural frequency of the spacecraft as its attached to the launcher. Moreover, the same thing has been done for the tanks and the natural frequency of the tanks relative to the spacecraft structure has been computed. Additionally for a more accurate natural frequency, a 2 degree of freedom spring system has been created for each propellant tank connected to the spacecraft and the natural frequency was calculated accordingly. For this section it was perceived that the current design of the spacecraft has a natural frequency that is larger than the minimum frequency set by the launcher (15 Hz) by a fair amount, this is the case even when considering the lowest natural frequency that has been computed in the 1 degree of freedom and the 2 degree of freedom (lowest natural frequency computed was 76.7 Hz in the axial direction).

Finally, the danger posed by micrometeoroids was analyzed. For the particle sizes that have a reasonable probability to hit the spacecraft during its mission it was found that they can penetrate the spacecraft walls. The biggest depth that particles could penetrate found was to be 8.168 mm, which cannot be mitigated by increased wall thicknesses. Therefore it is recommended to further research shielding such as whipple shields and implement them in the spacecraft to ensure mission success.

Recommendations

In the following, recommendations for a next refinement of the design are given:

1. The importance of the spherical part for the buckling and axial loads shall be investigated in the next design iteration.
2. The lateral loading shall be taken into account. It was neglected for now due to time constraints.
3. Different failure mode shall be investigated for a next more detailed design. This could include new failure criteria such as Tresca criterion and others.
4. In order to get a more accurate natural frequency of the spacecraft it is recommended to model the spacecraft and the tanks as a spring system of 3 degrees of freedom instead of repeating the calculations for 2 degrees of freedom twice (once for each propellant tank).
5. The analysis of the dynamic studies should include vibrations in the lateral directions as well since the launcher specifies a minimum frequency for the lateral direction.
6. It is recommended to further research shielding such as whipple shields and implement them in the spacecraft to ensure mission success and avoid failure due to micrometeoroids.
7. A further study shall be conducted to map the affects of sloshing and fuel loads.

References

[1] B. group, *Design of the juice orbiter*, 2020.

[2] B. Zandbergen, *AE1222-II: Aerospace Design & Systems Engineering Elements I*.

[3] R. Alderliesten, "Introduction to aerospace structures and materials," 2018. DOI: 10.5074/T.2018.003. [Online]. Available: https://textbooks.open.tudelft.nl/index.php/textbooks/catalog/book/15.

[4] B. group, *Design of the juice orbiter*, 2020.

[5] M. Inc. (2020). "Spacecraft propellant tanks," [Online]. Available: https://www.moog.com/products/propulsion-controls/spacecraft/spacecraft-propulsion-components/propellant-tanks.html.

[6] M. Aerospace. (2020). "Spacecraft propellant tanks," [Online]. Available: https://www.mt-aerospace.de/downloadcenter.html?file=files/mta/tankkatalog/MT-Tankkatalog_01b_4-3_03.pdf.

[7] M. Steel. (2019). "Why stainless steel is essential for the aerospace industry," [Online]. Available: https://www.marlinwire.com/blog/why-you-should-use-stainless-steel-for-aerospace-applications.

[8] A. aerospace specification metal inc. (1996). "Aluminum 2024-t3," [Online]. Available: http://asm.matweb.com/search/SpecificMaterial.asp?bassnum=MA2024T3.

[9] . L. Tianjin TEDA Ganghua Trade Co. (2020). "Aluminum alloy sheet t4 t3 aluminum sheet price per kg," [Online]. Available: https://m.made-in-china.com/product/Aluminum-Alloy-Sheet-2024-T4-T3-Aluminum-Sheet-Price-Per-Kg-777315092.html.

[10] A. aerospace specification metal inc. (1996). "Titanium ti-6al-4v (grade 5), annealed," [Online]. Available: http://asm.matweb.com/search/SpecificMaterial.asp?bassnum=MTP641.

[11] T. A. Ti-6Al-4V. (2020). "Ferrous and non ferrous alloy piping," [Online]. Available: http://www.metalspiping.com/titanium-alloy-ti-6al-4v.html#:~:text=Price%5C%20per%5C%20Kg,4V%5C%20bar(ASTM%5C%20B348%5C%20Gr. (visited on 11/24/2020).

[12] A. aerospace specification metal inc. (1996). "Aisi type s15500 (15cr-5ni) precipitation hardening stainless steel transverse direction, intermediate location, condition h1150," [Online]. Available: http://asm.matweb.com/search/SpecificMaterial.asp?bassnum=MQM15AF.

[13] M. Prices. (2020). "Stainless steel," [Online]. Available: https://agmetalminer.com/metal-prices/stainless-steel/.

[14] F. MB. (2014). "Steel vs al: Steel still trumps aluminium for cost-efficient, sustainable car making," [Online]. Available: https://www.metalbulletin.com/Article/3330473/STEEL-VS-AL-Steel-still-trumps-aluminium-for-cost-efficient-sustainable-carmaking.html#:~:text=In%5C%20raw%5C%20materials%5C%20costs%5C%2C%5C%20aluminium,30%5C%25%5C%20more%5C%20expensive%5C%20than%5C%20steel. (visited on 12/04/2020).

[15] CNCLATHING. (2020). "Titanium vs aluminum, which metal to choose," [Online]. Available: https://www.cnclathing.com/guide/titanium-vs-aluminum-which-metal-to-choose-comparison-between-titanium-and-aluminum-cnclathing.

[16] e. a. W. K. Boyd. (1965). "Compatibility of materials with rocket propellants and oxidizers," [Online]. Available: https://apps.dtic.mil/dtic/tr/fulltext/u2/664058.pdf.

[17] F. D. Hess. (1967). "Studies of corrosion inhtbitors for nitrogen tetroxide," [Online]. Available: https://apps.dtic.mil/dtic/tr/fulltext/u2/664058.pdf.

[18] B. Zandbergen, *AE1222-II: Aerospace Design & Systems Engineering Elements I*.

[19] D. J. Inman, *Engineering Vibrations*, fourth. Pearson, 2019.

[20] U. L. Alliance, *Atlas V launch services User's Guide*. 2010.

[21] P. B. Babadzhanov and G. I. Kokhirova, "Densities and porosities of meteoroids," *Astronomy & Astrophysics*, vol. 495, no. 1, pp. 353–358, Dec. 2008. DOI: 10.1051/0004-6361:200810460. [Online]. Available: https://doi.org/10.1051/0004-6361:200810460.

[22] K. K. de Groh, B. A. Banks, S. K. Miller, and J. A. Dever, "Degradation of spacecraft materials," in *Handbook of Environmental Degradation of Materials*, Elsevier, 2018, pp. 601–645. DOI: 10.1016/b978-0-323-52472-8.00029-0. [Online]. Available: https://doi.org/10.1016/b978-0-323-52472-8.00029-0.

[23] ESA. (2020). "Hypervelocity impacts and protecting spacecraft," [Online]. Available: https://www.esa.int/Safety_Security/Space_Debris/Hypervelocity_impacts_and_protecting_spacecraft.

Python Code A

This appendix presents the python code used in chapter 2. First, the functions used are presented and then the main code is given.

```
import math
# Python WP5
# 5.3b

g = 9.80665 # Hoekstra RPZ
# Inputs
def pressure_thickness(R, p, stress_yield, v):
    t2 = p * R / stress_yield
    t1 = (1-v)/(2-v) * t2

    return t1, t2

def stress_pressure_spherical_cap(R, p, t_2):
    return p*R/t_2
def critical_stress_shell_buckling(material, R, L, t_1, p):
    ''' Get critical stress due to the shell buckling
        @Input: List of material properties: [E, v, stress_yield]
                Geometrical properties: R, L, t_1
        @Output: critical stress due to shell buckling'''
    E = material[0]
    v = material[1]
    Q = (p * (R/t_1)**2 )/E
    dummy_lambda = (12 * L**4 * (1-v**2))/(math.pi**4 * R**2 * t_1**2)
    lambda_minimumk = math.sqrt(dummy_lambda)
    k = lambda_minimumk + 12 * L**4 * (1-v**2) / (math.pi**4 * R**2 * t_1**2 *
    lambda_minimumk)
    critical_stress = (1.982-0.983 * math.exp(-23.14 * Q)) * k * E * math.pi**2 * t_1**2
    / (12*(1-v**2)*L**2)
    return critical_stress

def mass_fuelTankinitial(R, L, t_1, t_2, m_fuel, density):
    '''Get mass of the spacecraft:
        @Assumption: cylinder with spherical caps.
        @Input: R, L, t_1, t_2, attachment mass m_attachments.
        @Ouput: the mass of the fuel tank with attachment.'''

    mass_cylinder = 2 * math.pi * R * t_1 * L * density
    mass_1_cap = (4 * math.pi * R**2 * t_2 / 2) * density
    mass_total_caps = 2 * mass_1_cap

    return (mass_cylinder + mass_total_caps + m_fuel)
print(mass_fuelTankinitial(1, 1, 0.001, 0.001,0, 2700))

def eulerBuckling(R, t_1, L, materiallst):
   E= materiallst[0]
   I = 1/4 * math.pi * (R**4- (R-t_1)**4)
   A = math.pi * (R**2 - (R-t_1)**2)
   criticalstress = ((math.pi)**2 * E * I)/(A*L**2)
   return criticalstress

def massAttachments(M, m_attachwp4, n_attach):
    Fres_wp4 = math.sqrt(1643.2**2+(1643.2 + 950)**2+4929.5**2) # WP4 resultant force
    Fz = 5.5 * g * M # 5.5 is axial load factor
```

```
    Flat = 0.4 * g * M # 0.4 is lateral load factor
    Fres = math.sqrt(Fz**2+Flat**2)
    Fres_per_attach = Fres / n_attach
    Fres_ratio = Fres_per_attach / Fres_wp4

    m_attach = Fres_ratio * m_attachwp4
    totalattachmentmass = n_attach* m_attach
    return totalattachmentmass


###
def newtotalmass(M, n_attach, m_attachwp4,m_attachold):
    M = M - m_attachold* n_attach + totalattachmentmass(M, n_attach, m_attachwp4)
    return M
```

Listing A.1: Functions used for the iterations

In the following, the code in which the functions are used to perform the iteration is presented.

```
import math
from WP5Equ import *
import numpy as np
from operator import itemgetter
# We neglect stress from launch in spherical caps
# Keep mass of fuel and oxidizer the same
# WP5 main
g = 9.80665 #m/s/s

V = 0.575 # Given by WP2 fuel
p = 25 * 10**5 # Given by fuel requirement
m_fuel = 527.7 # kg, from fuel used
material = [113.8 * 10**9, 0.342, 880 * 10**6, "Ti-6Al-4V (Grade 5), annealed"] # [E, v,
    stress_yield, name]
rho = 4500# kg/m^3

n_attach = 5 # Constant from configuration
m_attachwp4 = 0.201 # kg from attachment WP4
m_SC_without_fuelTank = 2304-19.5-m_fuel# kg # # Or oxidizer

Lmax = 1.5 # m
parametersRootsMinimumR = [(4/3)*math.pi, math.pi*Lmax, 0, -V]
Rmin = np.roots(parametersRootsMinimumR)[2] # Use real root
R = Rmin.real #m Beginning iterations

max_chosen = (V * (3/(4 * math.pi)))**(1/3) - 0.01#m
### MAIN SCRIPT ###
lstDesigns = []
i = 0
while R < max_chosen:
    print(f"R = {R}m")
    for t_2 in np.arange(0.00001, 0.01, 0.00001): # iterate on thickness of spherical
    caps
        i += 1
        if i % 100 == 0:
            print(i)
        L = (V-(4/3)*math.pi*R**3)/(math.pi * R**2)
        t_1 = ((2-material[1])/(1-material[1]))*t_2
        A = 2 * math.pi * R * t_1 # Cross sectional area
        M = m_SC_without_fuelTank + mass_fuelTankinitial(R, L, t_1, t_2, m_fuel, rho)
        M_attachOld = 0
        diff = 1
        while diff > 10**(-5):
            M1 = M
            M_attachNew = massAttachments(M, m_attachwp4, n_attach)
            M += M_attachNew
            M -= M_attachOld
            M_attachOld = M_attachNew
```

```
            M2 = M
            diff = M2 - M1
            # print(M_attachNew)
        # print("Converged!")
        M_attach = M_attachNew
        # Buckling tests
        sigmaCR_shellBuckling = critical_stress_shell_buckling(material, R, L, t_1, p)
        # print(sigmaCR_shellBuckling)
        sigmaCR_eulerBuckling = eulerBuckling(R, t_1, L, material)
        # print(sigmaCR_eulerBuckling)
        drivingCRStress = min(sigmaCR_shellBuckling, sigmaCR_eulerBuckling, material[2])
        # print(f"driving stress = {drivingCRStress}")
        Fz = 5.5 * g * M # 5.5 is axial load factor
        stressAxial = Fz/A + p*R/(2*t_1) # Negligible lateral load
        if stressAxial <= drivingCRStress and material[2] >= stress_pressure_spherical_cap(R, p, t_2):
            m = 2 * math.pi * R * L * t_1 * rho + 4 * math.pi * R**2 * t_2 * rho + M_attach
            design = [R, L, t_1, t_2, m]
            # print(mass_fuelTankinitial(R, L, t_1, t_2, m_fuel, rho)+M_attachNew-m_fuel)
            lstDesigns.append(design)

    R += 0.001

#print(lstDesigns)
best_designs = sorted(lstDesigns, key = itemgetter(4))
print(best_designs[0])

print(f"OXYDIZER: For {material[3]}, the thickness of the cylindrical part t_1 is: {best_designs[0][2]}m"
      f"the thickness of the end caps t_2 is {best_designs[0][3]}m and the radius is {best_designs[0][0]}m"
      f"the length of the cylindrical part is {best_designs[0][1]}m."
      f"This gives a total mass of {best_designs[0][4]}kg.")
```

Listing A.2: Main code used for the iterations

Task Distribution B

Table B.1 presents the task distribution of the various deliverables present in the report.

Table B.1: Task distribution

Task	Made	Proofread
Summary	Niklas	Stefano, Sam
Introduction	Niklas	Stefano, Lorenz
5.1	Tarek, Stefano, Antonio	Sam, Jonatan
5.2	Niklas, Sam	Silvano, Jonatan, Stefano, Lorenz
5.3	Lorenz, Jonatan	Sam, Stefano
5.4	Jonatan, Lorenz, Niklas	Niklas, Stefano
5.5	Lorenz, Silvano, Tarek	Niklas, Sam, Jonatan, Antonio, Stefano
5.6	Jonatan, Tarek, Antonio	Lorenz, Jonatan
5.7	Niklas	Jonatan, Tarek
Conclusion	Niklas, Tarek, Stefano	Sam
Appendix A	Lorenz	